

## Experimental investigation and numerical predictions of the mean flow of a turbulent pure plume<sup>(\*)</sup>

M. BRAHIMI and DOAN-KIM-SON (POITIERS)

AN EXPERIMENTAL study of a turbulent pure plume is carried out. The determination of the velocity profiles is performed with a laser Doppler anemometer system. The flow field at the base of the plume is analysed. Of particular interest was the entrainment and intermittency in such flows. The plume was found to be strongly intermittent because of its sinuous structure with large-scale vortices. The numerical predictions presented take into account the intermittency factor through a modified eddy-viscosity.

Wykonano badania eksperymentalne nad burzliwymi pióropuszcami gazowymi analogicznymi do obłoków dymu unoszących się nad źródłem ognia. Profile prędkości przepływu określono za pomocą metod laserowej anemometrii dopplerowskiej. Przeanalizowano pole prędkości u podstaw pióropusza. Zwrócono szczególną uwagę na zjawiska pulsacji przepływu i unoszenia. Przepływ okazuje się wysoce pulsacyjny ze względu na swą wężykowatą strukturę i wiry dużych rozmiarów. Obliczenia numeryczne uwzględniają zjawisko pulsacji za pomocą zmodyfikowanego współczynnika lepkości wirowej.

Проведены экспериментальные исследования турбулентных газовых столбов, аналогичных облакам дыма поднимающимся над источником огня. Профили скорости течения определены при помощи методов доплеровской лазерной анемометрии. Проанализировано поле скорости у основы столба. Обращено особенное внимание на явления пульсации течения и уноса. Течение оказывается высоко пульсационным из-за его змееобразной структуры и вихрей больших размеров. Численные расчеты учитывают явление пульсации при помощи модифицированного коэффициента вихревой вязкости.

### 1. Introduction

BECAUSE of their fundamental and practical interest, turbulent plumes have been the subject of investigation for a long time. This flow situation is in fact frequently encountered in thermal processes, in nature and it is created by fires.

The state of knowledge on turbulent plumes has been summarized by TURNER [1] and CHEN and RODI [2], among others. A critical examination of these works shows that few investigations have been concerned with pure turbulent plumes (without initial momentum). Unfortunately, these studies are limited to the determination of the self-preserving region characteristics and do not deal with the intermittency phenomenon. In order to understand entrainment and mixing processes in such flows, the analysis of their different stages of development is of importance. On the other hand, it is obvious that, although mathematically attractive, the time-averaged turbulent plume concept does gross injustice

(\*) Paper given at XVII Symposium on Advanced Problems and Methods in Fluid Mechanics, Sobieszewo, 2-6 September 1985.

to the physics of the phenomenon. A turbulent plume does not rise straight up into the air with a fixed shape like jets but presents large-scale vortices.

In this paper the behaviour of a pure turbulent plume is analysed in its different stages with the purpose of understanding entrainment and intermittency of such flows. The results of numerical predictions which take into account the intermittency factor are compared with the experimental data. The mathematical model relies on the mixing-length hypothesis with variable thermophysical properties of the fluid.

## 2. Experimental apparatus and measurement techniques

The plume source is a hollow portion of a stainless steel sphere heated up to  $T_p \approx 500^\circ\text{C}$  (Fig. 1). Because of the sensitivity of the turbulent plume to weak draughts, it is necessary to keep the surrounding atmosphere still. That is why the source is put in a small room with sufficient dimensions to consider the environment as unlimited.

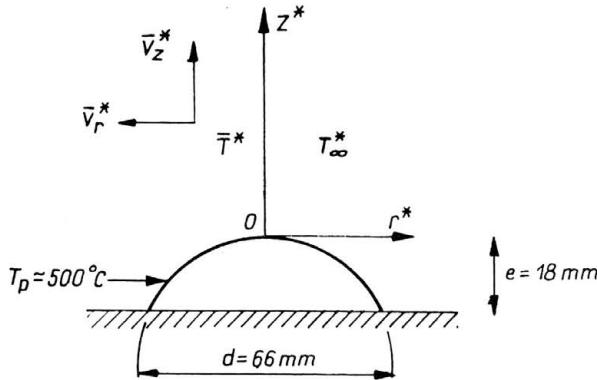


FIG. 1. Coordinate system.

The temperature measurements were performed with a probe operating as a resistance thermometer [3]. The effect of the source radiations on the temperature measurements was estimated and found negligible. In the present work a laser Doppler anemometer (L.D.A.) system was used to obtain velocity profiles. This technique presents some advantages as compared to hot wire anemometry. Due to the fact that the L.D.A. method does not suffer directional ambiguity, it is well adapted to the freely rising flow studied. Low radial velocities can then be measured.

The turbulent plume was seeded with droplets of vegetable oil produced by a seeding generator, and added into the flow long before measurements were made. These particles allow us to obtain good signals and satisfactory data rates. One may estimate the accuracy of velocity measurements using tracer particles. The difference between particle and fluid speeds, with regard to the dimension and nature of the particle, is found to be less than 10% for velocities lower than 10 cm/s and less than 1% for velocities higher than 10 cm/s [4].

Temperature and velocity signals were stored in a data acquisition device where they are digitized and recorded on magnetic tapes for further statistic processing. Each signal was recorded during 6 minutes with an acquisition frequency of 100 Hz.

### 3. Analysis

The problem of the rising air column above a strongly heated source is considered to be a turbulent free convection problem. The classical boundary-layer approximations are assumed but the viscous and molecular transport of momentum and heat are not neglected with regard to the turbulent transport. With these assumptions the equations for axisymmetric turbulent plume can easily be derived (see Fig. 1 for the coordinate system):

$$(1) \quad \frac{\partial}{\partial z} (r\bar{\rho}\bar{V}_z) + \frac{\partial}{\partial r} (r\bar{\rho}\bar{V}_r) = 0,$$

$$(2) \quad r\bar{\rho}\bar{V}_z \frac{\partial \bar{V}_z}{\partial z} + r\bar{\rho}\bar{V}_r \frac{\partial \bar{V}_z}{\partial r} = r\bar{\rho}\bar{T} + \frac{1}{\sqrt{Gr_0}} \frac{\partial}{\partial r} \left[ r(\bar{\mu} + \mu_t) \frac{\partial \bar{V}_z}{\partial r} \right],$$

$$(3) \quad r\bar{\rho}\bar{V}_z \frac{\partial \bar{T}}{\partial z} + r\bar{\rho}\bar{V}_r \frac{\partial \bar{T}}{\partial r} = \frac{1}{\sqrt{Gr_0}} \cdot \frac{1}{Pr_0} \cdot \frac{\partial}{\partial r} \left[ r(\bar{\lambda} + \lambda_t) \frac{\partial \bar{T}}{\partial r} \right].$$

All variables are in a dimensionless form:

length

$$r = \frac{r^*}{L}, \quad z = \frac{z^*}{L} \quad (\text{length} = \text{height of the plume});$$

velocity

$$\bar{V}_z = \frac{\bar{V}_z^*}{V_c}, \quad \bar{V}_r = \frac{\bar{V}_r^*}{V_c} \quad \left( V_c = \left( g.l. \frac{T_p^* - T_\infty^*}{T_\infty^*} \right)^{1/2} \right);$$

temperature:

$$\bar{T} = \frac{\bar{T}^* - T_\infty^*}{T_p^* - T_\infty^*},$$

where the subscript “\*” denotes a dimensional variable.

The thermophysical properties of the fluid: density, thermal conductivity and dynamic viscosity, respectively, are evaluated from their state equations:

$$\bar{\rho} = \frac{\bar{\rho}^*}{\rho_\infty^*} = \bar{\rho}(\bar{T}), \quad \bar{\lambda} = \frac{\bar{\lambda}^*}{\lambda_\infty^*} = \bar{\lambda}(\bar{T}), \quad \bar{\mu} = \frac{\bar{\mu}^*}{\mu_\infty^*} = \bar{\mu}(\bar{T}).$$

and the coefficients  $Gr_0$ ,  $Pr_0$  and  $Fr_0$  are defined as follows:

$$Gr_0 = \frac{gL^3}{\nu_\infty^{*2}} \cdot \frac{T_p^* - T_\infty^*}{T_\infty^*} \quad (\text{Grashoff number}),$$

$$\text{Pr}_0 = \frac{\mu_\infty^* C_p^*}{\lambda_\infty^*} \quad (\text{Prandtl number}),$$

$$\text{Fr}_0 = \frac{V_c^2}{gL} = \frac{T_p^* - T_\infty^*}{T_\infty^*} \quad (\text{Froude number}).$$

The solution of the set of equations above depends on two independent variables ( $r, z$ ) and three parameters  $\text{Gr}_0, \text{Pr}_0$  and  $\text{Fr}_0$ , the latter appearing in the state equation of  $\bar{\rho}, \bar{\lambda}, \bar{\mu}$  if written as

$$\bar{\phi} = (1 + \text{Fr}_0 \bar{T})^{m_\phi}, \quad \bar{\phi} = \bar{\rho}, \bar{\lambda}, \bar{\mu}.$$

The results are given for  $\text{Pr}_0 = 0.7$  and  $\text{Fr}_0 = 1.57$  which for  $T_\infty^* = 27^\circ\text{C}$  corresponds to a  $500^\circ\text{C}$  temperature difference between the source and ambient fluid.

In this temperature interval, appropriate values for the exponents  $m_\phi$  are found to be  $m_\lambda = 8/9, m_\mu = 3/4, m_\rho = -1$ . The temperature dependence of  $\bar{\rho}, \bar{\lambda}$  and  $\bar{\mu}$  is then calculated with a better than 1% accuracy compared with their standard tabulated values.

Previous equations (1) ~ (3) show that an eddy viscosity model is utilised in the present study. The simpler theory of PRANDTL [5] presumes a constant eddy viscosity at each flow cross section, varying only with the longitudinal distance along the flow. It is known that Prandtl's simpler theory can be confidently applied to the core of jets and wakes [6]. The advantage of this simpler theory is that there is no infinite curvature of the velocity profile on the flow axis when compared to mixing-length theory calculation. But this latter is expected to give better agreement with experimental results near the edge of the flow. This performance is due to the significant variation of turbulent transport coefficients well represented by the mixing-length theory. In the present paper we have used, as a first step, the simpler theory of Prandtl but in order to predict better results we have taken into account the strong intermittent character of the plume which attenuates the turbulent mixing. The eddy viscosity is therefore weighted by the intermittency factor  $\gamma$  as follows:

$$v_t = l_m \bar{V}_{z \text{ axc}} \cdot \gamma \cdot \sqrt{\text{Gr}_0},$$

where  $l_m$  is a mixing-length characteristic. We define the half-width  $l_v$  of the plume as the 1/2 points of the velocity profile. Then we propose the following expression of kinematic eddy viscosity for turbulent plumes:

$$v_t = 0.075 l_v \cdot \bar{V}_{z \text{ axc}} \cdot \gamma \cdot \sqrt{\text{Gr}_0}.$$

If  $\text{Pr}_t$  denotes the turbulent Prandtl number, the eddy diffusivity can be written as

$$\lambda_t = \frac{\text{Pr}_0}{\text{Pr}_t} \cdot v_t.$$

Since measurements of  $\gamma$  are made in the established region of the plume, calculations at lower altitudes are performed without  $\gamma$ . At these altitudes the flow is rather in a transitional regime where viscous and molecular transport of momentum and heat are prevailing.

The system of equations (1) ~ (3) is parabolic and marching integration can be used in the streamwise coordinate  $z$ . The system is solved numerically by a method based on a Crank-Nicholson scheme.

The boundary conditions are:

$$\begin{aligned} \frac{\partial \bar{V}_z}{\partial r} = 0, \quad \bar{V}_r = 0, \quad \frac{\partial \bar{T}}{\partial r} = 0 \quad \text{at} \quad r = 0, \\ \bar{V}_z = 0, \quad \bar{T} = 0, \quad V'_r = V'_z = T' = 0 \quad \text{at} \quad r \rightarrow \infty, \\ \bar{V}_z = \bar{V}_{0z}(r), \quad \bar{T} = \bar{T}_0(r) \quad \text{at} \quad z = 0. \end{aligned}$$

Calculations begin at  $z^* = 5$  mm with the experimental profiles  $\bar{V}_z^*(5, r^*)$  and  $\bar{T}^*(5, r^*)$ . The turbulent Prandtl number is taken equal to 0.75. The previous value is commonly used for the calculations of free turbulent flows [7].

#### 4. Results and discussion

The plume structure is presented in Fig. 2. One observes on this photo the presence of large-scale vortices which extend across the whole width of the plume, their charac-



FIG. 2. Pure plume structure.

teristic lengths increasing with height. As explained by LUMLEY [8], the plume column is subjected to axial and radial compressions due to vertical and horizontal temperature gradients respectively. With such properties, the straight plume becomes analogous to an elastic column [9]. This mechanism produces large-scale vortices as shown by Fig. 2. It is obvious that the intermittency will reach the central region of the plume. Measurements of the intermittency factor  $\gamma$  in the self-preserving region are presented in Fig. 3. We

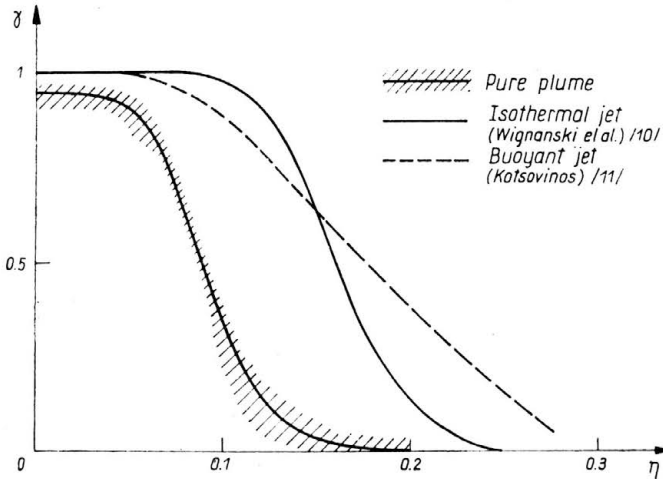


FIG. 3. Intermittency factor.

note a scatter in the data due to the manual method used to determine  $\gamma$  [3]. The intermittency factor along the axis of the turbulent plume is found to be less than one which confirms the behaviour of the visualized large eddies. The corresponding results of both isothermal jet [10] and plume with initial momentum [11] are reported in Fig. 3 for purposes of comparison and exhibit an intermittent character less important than that of the turbulent pure plume studied. This difference is probably explained by the fact that the smaller vortices in a jet are different in structure and they do not reach the central jet region. In order to take into account the intermittent character in a mathematical model in the way presented previously, it is worth expressing  $\gamma$  in an analytical form. According to TOWNSEND'S work [12], the intermittency factor can be written as

$$\gamma = \left[ 1 + \frac{\eta^4}{\eta_0^4} \right]^{-1} \quad \text{with} \quad \eta_0 = 0.09 \quad \text{and} \quad \eta = r/(z - z_0),$$

$z_0$  denotes the position of the virtual origin of the plume.

The results of numerical predictions of the vertical mean velocity in the established region of the plume are presented in Fig. 4. A good comparison is obtained with experimental data even at the plume edge where the flow is strongly influenced by the ambient fluid. We note that the experimental profiles are self-similar and they are commonly assumed to be Gaussian [13, 14, 15]. But the function of the form  $(1 + A\eta^2)^{-2}$  appears to fit better the experimental data for  $\eta > 0.1$  (Fig. 4). The width-scale  $l$  is defined in terms of the 1/2 points of the Gaussian curve. Hence we obtain the following spreading law for the velocity field:  $l_v^* = 0.103(Z^* - Z_0^*)$ .

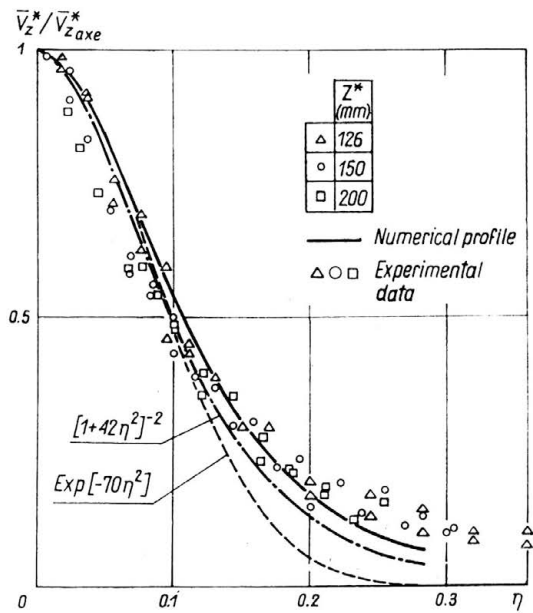


FIG. 4. Velocity profiles (self-preserving region).

The spread angle is seen to be lower than those observed by other authors [2]. It is worth noting that they have used different generating plume systems and they have also determined the velocity profiles by using techniques which suffer directional ambiguity.

Several investigations have been concerned with the entrainment phenomenon [11, 16, 17]. The entrainment coefficient is quite important and is related to the spread angle as shown below:

$$\alpha = \frac{5}{6} \left( \frac{2}{\text{Ln} 2} \right)^{1/2} \frac{dl_v^*}{dZ^*},$$

$\alpha$  characterizing the lateral mass transport and playing an important role in integral modelization of plumes [18, 19]. The previous relation allows the evaluation of  $\alpha$  for different plume sources. The values obtained are reported in the table below. One observes that plumes present an entrainment two times more effective than that of jets. As mentioned previously, large-scale vortices of plumes engulf an ambient irrotational fluid. Since the scale of the large vortices is much smaller in a jet than in a plume, it can be argued that the plume achieves larger entrainment.

At this stage, we have analysed the established region of the plume. At lower altitudes the mechanism of entrainment is expected to be strong because of the zero initial momentum. The fluid entrained from the environment must supply the one transported downstream by the flow. This transport is related to the radial velocity.

We have reported in Fig. 5 three characteristic profiles of the mean radial velocity at early stages of the plume. It appears that the entrainment is strong at the base of the plume and then decreases as we rise up according to radial velocity values.

Numerical predictions are seen to be satisfactory, although boundary layer approximations are gross at the base of the flow because of the mean radial velocity magnitude.

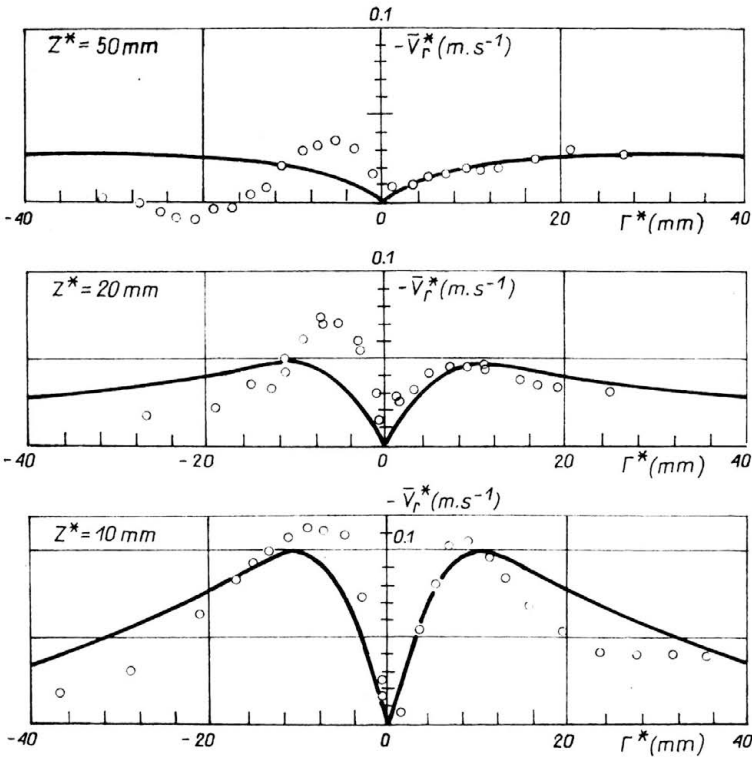


FIG. 5. Mean radial velocity distribution,  $\circ$  experimental data, — numerical calculation.

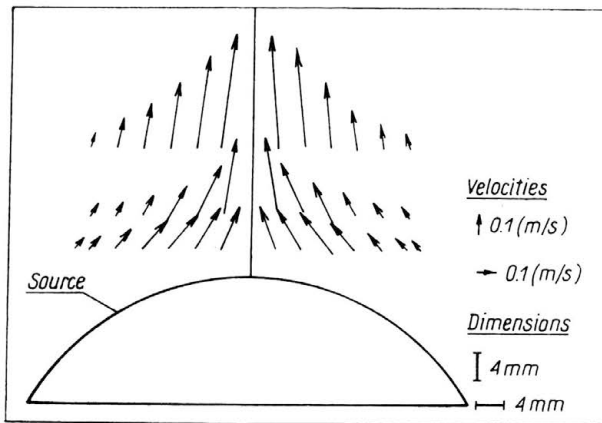


FIG. 6. Velocity field above the source.

Figure 6 shows the velocity field just above the source. One observes that the ambient air inflowing narrows the base of the plume and so creates strong radial gradients. Another feature of the flow at early stages is the increasing of mean vertical velocity. This acceleration results from the action of buoyancy forces. These forces are important as shown by the high centerline excess temperature at lower altitudes (see Fig. 7).



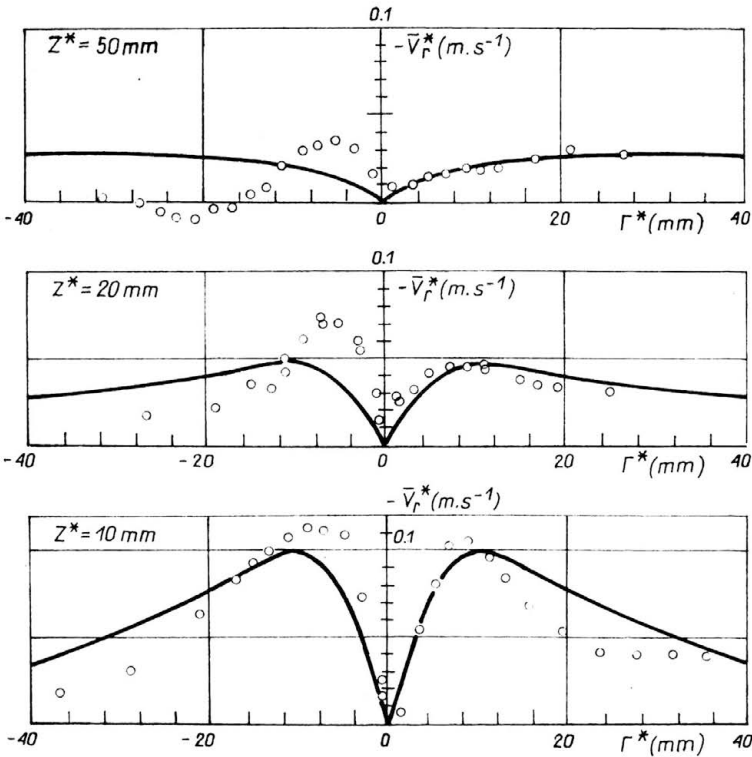


FIG. 5. Mean radial velocity distribution,  $\circ$  experimental data, — numerical calculation.

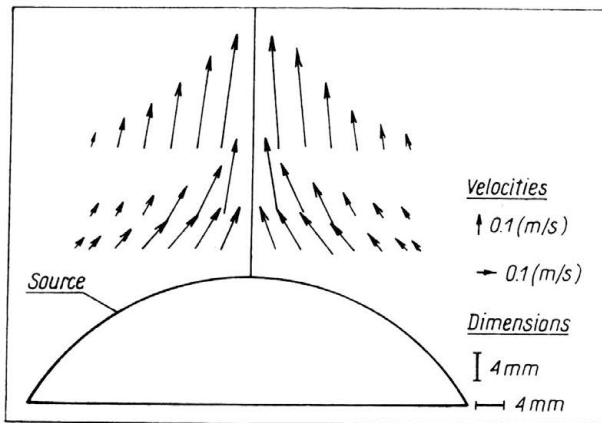


FIG. 6. Velocity field above the source.

Figure 6 shows the velocity field just above the source. One observes that the ambient air inflowing narrows the base of the plume and so creates strong radial gradients. Another feature of the flow at early stages is the increasing of mean vertical velocity. This acceleration results from the action of buoyancy forces. These forces are important as shown by the high centerline excess temperature at lower altitudes (see Fig. 7).

Table 1.

Authors	Plume sources	$\alpha$
Present study	Pure plume (portion of sphere)	0.15
GEORGE and al. [15]	Plume issued from heated jet	0.16
NAKAGOME and HIRATA [14]	Pure plume (heated disc)	0.17
ROUSE and al. [13]	Flame	0.12
RICOU and SPALDING [16]	Isothermal jet	0.08

## References

1. J. S. TURNER, *Ann. Rev. Fluid Mech.*, **1**, 29-44, 1969.
2. C. J. CHEN and W. RODI, *Vertical turbulent buoyant jets*, Pergamon Press, Oxford, U. K., 1980.
3. DOAN-KIM-SON, Thèse de Doctorat d'Etat, Université de Poitiers 1977.
4. C. RENAULT, Thèse de Docteur-Ingénieur, Université de Poitiers, 1983.
5. L. PRANDTL, *Z. Angew. Math. Mech.*, **22**, p. 241, 1942.
6. C. S. YIH, *Phys. Fluids*, **20**, 8, 1234-1237, 1977.
7. F. TAMANINI, *Symp. Turb. Shear Flows*, Pennsylvania, U.S.A., pp. 6.29-6.37, 1977.
8. J. L. LUMLEY, *Phys. Fluids*, **14**, 2537-2538 1971.
9. A. BEJAN, *Wärme-Stoffübertragung*, **16**, 4, 237-242, 1982.
10. I. WIGNANSKI and M. FIELDER, *J. Fluid Mech.*, **38**, 577-612, 1969.
11. N. E. KOTSOVINOS, *J. Fluid Mech.*, **81**, 45-62, 1977.
12. A. A. TOWNSEND, *Austr. J. Scient. Res.*, **2**, 4, 451-468, 1949.
13. H. ROUSE, C. S. YIH and H. W. HUMPHREYS, *Tellus*, **4**, 201-210, 1952.
14. H. NAKAGOME and M. HIRATA, *Proc. Int. Sem. Turb. Buoy. Conv.*, Dubrovnik, Yug., 361-372, 1976.
15. W. K. GEORGE, R. L. ALPERT and F. TAMANINI, *Int. J. Heat and Mass Transfer*, **20**, 11, 1145-1154, 1977.
16. F. P. RICOU and D. B. SPALDING, *J. Fluid Mech.*, **11**, 21-32, 1961.
17. E. J. LIST and J. IMBERGER, *J. Hyd. Div. A.S.C.E.*, **99**, 1461-1474, 1973.
18. B. R. MORTON, J. S. TURNER and G. I. TAYLOR, *Proc. Roy. Soc.*, **234A**, 1-23, 1956.
19. J. S. TURNER, *Buoyancy effects in fluids*, Camb. Univ. press, London, U.K., 1973.

LABORATOIRE DE THERMIQUE DE L'E.N.S.M.A., POITIERS, FRANCE.

Received September 10, 1985.